Journal of The Korean Astronomical Society
39: 1 ∼ 6, 2006

arXiv:astro-ph/0612063v1 4 Dec 2006

NEAR-INFRARED PHOTOMETRY OF THE STAR CLUSTERS IN THE DWARF IRREGULAR GALAXY IC 5152

Jaemann Kyeong[1] , Eon–Chang Sung[1] , Sang Chul Kim[1] , Sangmo Tony Sohn[2,3] and Hyun–Il Sung[1]
[1]Korea Astronomy & Space Science Institute, Taejon 305-348, Korea
E-mail: jman,ecsung,sckim,hisung@kasi.re.kr
[2]Center for Space Astrophysics, Yonsei University, Seoul 120-749, Korea
[3]Space Astrophysics Lab, California Institute of Technology, MC 405-47, 1200 East California Boulevard, Pasadena, CA 91125
E-mail: tonysohn@srl.caltech.edu
(Received Nov. 16, 2006; Accepted Dec. 1, 2006)

ABSTRACT

We present JHK-band near-infrared photometry of star clusters in the dwarf irregular galaxy IC 5152. After excluding possible foreground stars, a number of candidate star clusters are identified in the near-infrared images of IC 5152, which include young populations. Especially, five young star clusters are identified in the $(J-H, H-K)$ two color diagram and the total extinction values toward these clusters are estimated to be $A_V = 2-6$ from the comparison with the theoretical values given by the Leitherer et al. (1999)'s theoretical star cluster model.

Key words : galaxies: individual (IC 5152) — galaxies: dwarf irregular galaxies — galaxies: star clusters — galaxies: photometry - infrared: galaxies

I. INTRODUCTION

Since the discovery of new Milky Way satellite galaxies (e.g., Ursa Major dwarf spheroidal galaxy (Willman et al. 2005), Canes Venatici dwarf galaxy (Zucker et al. 2006a), Bootes dwarf galaxy (Belokurov et al. 2006), Ursa Major II dwarf spheroidal galaxy (Zucker et al. 2006b)) and new M31 satellite galaxies (e.g., Andromeda IX dwarf spheroidal galaxy (Zucker et al. 2004), Andromeda X dwarf spheroidal galaxy (Zucker et al. 2006c)), the number of dwarf galaxies in the Local Group has been increased to well over 30 (Grebel 2000). The dwarf galaxies are the most abundant type of galaxy in groups and clusters and the building blocks of more massive galaxies. Furthermore the intrinsic properties of dwarf galaxies, such as mass, density, and gas content, are likely to affect the star formation history and chemical enrichment. Therefore, the understanding of the properties of dwarf galaxies provides clues on the galaxy formation processes.

IC 5152 (=IRAS 21594–51, ESO 237-27), a dwarf irregular galaxy (Sdm IV−V), is one of the best objects available to study starbursts due to its rather close distance. On the other hand, a very bright star (HD 209142, $V = 7.9$, $K_s = 7.14$) in the north-western part of the galaxy makes it difficult to obtain deep exposures. Basic information of IC 5152 is summarized in Table 1.

It has been controversial whether IC 5152 is a member of the Local Group or not. Sandage (1986) estimated a distance modulus of $(m-M)_0 = 26$ from the brightest stars in this galaxy, and van den Bergh (1994) pointed out that this distance estimate is too uncertain to find the possibility of the Local Group membership. Zijlstra & Minniti (1999) found the distance modulus of IC 5152 to be $(m-M)_0 = 26.15 \pm 0.2$ using VI color-magnitude diagram (CMD) and red giant branch (RGB) tip method. But their photometry is not so deep to determine the RGB tip magnitude. Recently, using the HST snapshot survey of nearby galaxies, Karachentsev et al. (2002) found the accurate magnitude of the tip of the RGB (TRGB) of IC 5152 to be I(TRGB)= 22.58 ± 0.16 mag and derived the distance to be 2.07 ± 0.18 Mpc, equivalent to $(m-M)_0 = 26.58 \pm 0.18$, therefore, it is located at the outskirts of the Local Group.

The brightest H II region #A has been known in IC 5152 and several other H II regions are known in the disk of this galaxy (Hidalgo-Gámez & Olofsson 2002). IC 5152 is also an H I rich dwarf (Buyle et al. 2006). The H I image of the galaxy shows that H I gas is spread out on the face of IC 5152. This suggested that there should be many newly formed young stellar populations on the disk. The young populations are also contained in the massive young clusters which are hardly seen on optical images due to surrounding gas clouds.

Light at near-infrared wavelengths is less affected by dust absorption than at visible wavelengths($A_K = 0.1A_V$), making it easier to probe the heavily obscured star forming regions and detect young clusters.

Since the data used in this study do not have enough angular resolution to detect individual stars of IC 5152,

Corresponding Author: J. Kyeong

Table 1. Basic Information of IC 5152

Parameter	Information	Reference
$\alpha_{J2000.0}$, $\delta_{J2000.0}$	$22^h\ 02^m\ 41.^s5$, $-51^\circ\ 17'\ 47''$	NASA/IPAC Extragalactic Database
l, b	$343.^\circ92$, $-50.^\circ19$	NASA/IPAC Extragalactic Database
Type	Sdm IV–V	Sandage & Bedke 1985
Foreground reddening, $E(B-V)$	0.00 mag	Zijlstra & Minniti 1999
Diameter	2.1 kpc	Huchtmeier & Richter 1986
Minor to major axis ratio of the disk, $(b/a)_{disk}$	0.6	Sandage & Bedke 1985
Inclination, i	55°	Huchtmeier & Richter 1986
Distance modulus, (m-M)$_0$	26.58 ± 0.18 mag	Karachentsev et al. 2002
Distance, d	2.07 ± 0.18 Mpc ($1'' = 10.0$ pc)	Karachentsev et al. 2002
Absolute total magnitude, M_B	-14.8	Huchtmeier & Richter 1986
Radial velocity w.r.t. Local Group centroid, V_{LG}	$+53$ km s^{-1}	Huchtmeier & Richter 1986
Metallicity of the disk, $Z_{\rm disk}$	0.002	Skillman, Kennicutt, & Hodge 1989
Total mass-to-light ratio, (M_T/L_B)	3.5	Zijlstra & Minniti 1999
Number of candidate star clusters with $K \leq 16.6$	20	This study
Number of candidate young star clusters	5	This study

the goal of this paper is to find star clusters and investigate their properties. Especially, young star clusters with heavy reddening are investigated using the near-infrared wavelength characteristics.

This paper is composed as follows. We describe our near-infrared observations and data reduction in Section II. Section III present the results and analyses on star clusters in IC 5152 and a summary is given in Section IV.

II. NEAR-INFRARED OBSERVATIONS AND DATA REDUCTION

JHK_n images of IC 5152 were obtained on the night of UT 2002 June 30 using the 2.3 m telescope and the infrared (IR) camera CASPIR (Cryogenic Array Spectrometer/Imager) at the Siding Spring Observatory. A gray-scale map of the K_n-band CASPIR image of IC 5152 is displayed in Figure 1. The gain and readout noise of CASPIR are 9 e$^-$/ADU and 50 electrons, respectively. CASPIR uses 256×256 InSb detector and the pixel scale is $0\farcs50$ pixel^{-1}, which gives the field of view of $2\farcm1 \times 2\farcm1$. In order to get high signal-to-noise ratio, a total of 9 frames with 5 s exposure and 12 cycles were obtained, which means that the combined image is a result of combining 108 frames of the same exposure. The bias frames were frequently obtained over the night because the bias level was known to vary throughout the night (McGregor 1995). Also, in order to remove possible detector instability and temporal changes of the bright IR background, nearby sky frames ($10'$ away from IC 5152) were taken with the same exposure time.

The instrument characteristics and the IR sky of strong signal and rapid variability, makes the reduction procedure of near-IR data more complex than that of optical CCD data. First, the raw data had to be linearized to recover the low and high intensity information accurately according to the formula given by McGregor (1995). Then the bias and dark frames obtained just before and after each object frame were subtracted. The median combined sky frame was subtracted from the object frame. Finally, the data images are flattened by dome flats. Dome flats were obtained for each filter by differencing exposures with the flatfield lamp on and off, and several such frames were combined to form the final dome flat for each filter.

We used the point spread function (PSF) fitting packages of DAOPHOT II and ALLSTAR for the photometry. Stars of different frames were matched by DAOMATCH/DAOMASTER routines (Stetson 1993). For each frame, several isolated unsaturated stars were used to construct a good model PSF. Aperture corrections were made using the program DAOGROW (Stetson 1990) for which we used the same stars used in the PSF construction.

In order to transform instrumental magnitudes to the standard system, we observed 12 SAAO photometric standard stars given by Carter & Meadows (1995) throughout the observing run. We derived the transformation equations between our instrument magnitudes and the standard values J, H, K as following;

$$\begin{aligned} J &= j + 18.87(\pm0.10) - 0.16(\pm0.09) * X_j - \\ &- \ 0.09(\pm0.07) * (J-K) \\ H &= h + 18.69(\pm0.03) - 0.14(\pm0.09) * X_h + \\ &+ \ 0.20(\pm0.07) * (J-H) \\ K &= k + 17.79(\pm0.05) - 0.07(\pm0.13) * X_k + \\ &+ \ 0.13(\pm0.09) * (J-K) \end{aligned}$$

where j, h and k are instrumental magnitudes, X_j, X_h and X_k are airmasses at each bandpass. The residuals of standard star calibration were 0.10, 0.03, and 0.06 mag for J, H, and K filter, respectively. We can check the photometric calibration accuracy using a common star observed by CASPIR (the second bright star in the K-band CASPIR frame at X=175.8,

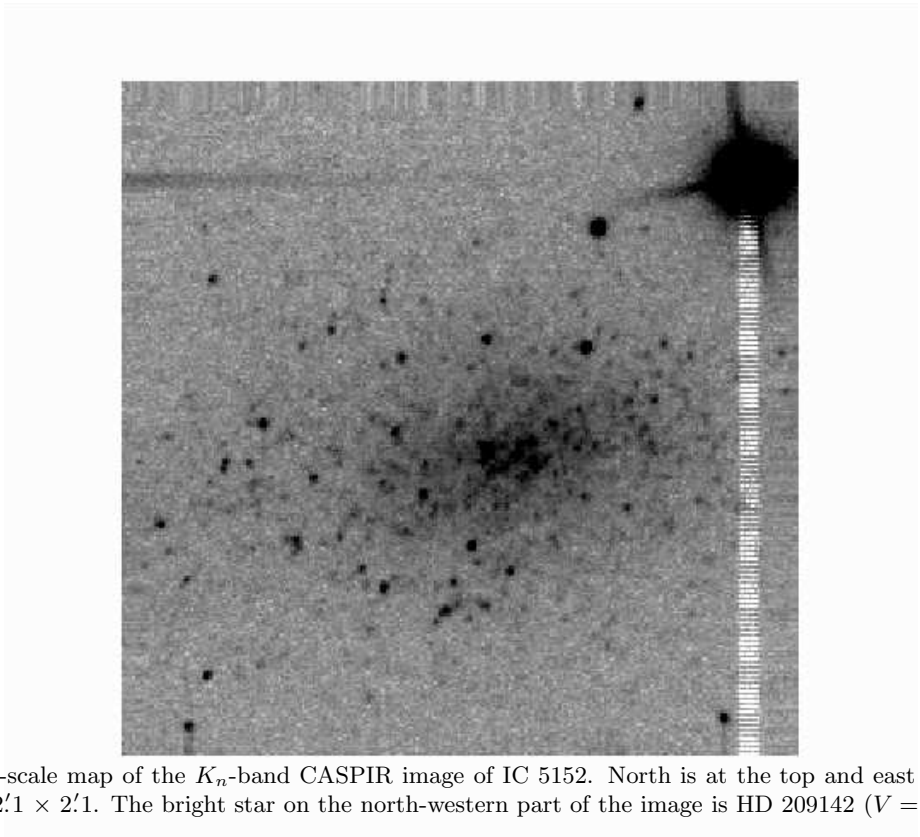

Fig. 1.— Grey-scale map of the K_n-band CASPIR image of IC 5152. North is at the top and east is to the left. The size of the field is $2\farcm1 \times 2\farcm1$. The bright star on the north-western part of the image is HD 209142 ($V = 7.9$, $K_s = 7.14$).

Y=198.2) and 2MASS Point Source Catalog (Cutri et al. 2003). The comparison gives a good agreement in J and H-bands within the photometric errors. However, in the K-band, there is somewhat big difference of Δ(Ours−2MASS)=0.13 mag due to the different filter systems used, K_n and K_s.

III. STAR CLUSTERS IN IC 5152

(a) Contamination of Foreground Stars

We adopted the distance modulus of IC 5152 $(m - M)_0 = 26.6 \pm 0.2$ (Karachentsev et al. 2002) and the reddening toward this galaxy $E(B-V) = 0.0$ (Burstein & Heiles 1984; Zijlstra & Minniti 1999). The color-magnitude diagrams for all the objects in IC 5152 are shown in Figure 2.

Since the detected objects are not resolved, they could be contaminated by foreground stars. Likely foreground stars cannot be identified using near-IR CMD and/or two-color diagram because their near-IR colors and brightnesses are not separated from those of the IC 5152 members. Therefore, we identified the foreground stars using another catalog. As pointed out by Zijlstra & Minniti (1999) already, $2 \sim 3$ foreground stars are expected in our observed field of $2\farcm1 \times 2\farcm1$ with $V \leq 21$ mag from the Galactic star count model of Ratnatunga & Bahcall (1985). One foreground star except the brightest star (HD 209142) at the upper right corner of the image can be identified using 2MASS Point Source Catalog. A comparison with sources in the 2MASS Point Source Catalog confirms the second bright star(α(J2000) = $22^h\ 02^m\ 39.^s4$, δ(J2000) = $-51^\circ\ 17'\ 05\farcs6$, $J = 14.28$, $H = 13.66$, $K_s = 13.39$).

We also can identify the foreground stars in the blue plate (IIIaO + GG38) of NED (NASA/IPAC Extragalactic Database) after subtracting out the diffuse body of the galaxy. A point-source like object is found during this process at X=28 and Y=29 of our K-band image with J=16.89, H=16.09, and K=15.86 mag. Only very faint background galaxies might be included in our small field.

(b) Star Clusters

Using the magnitude of the brightest blue supergiants, $M_K = -10$ mag (Rozanski & Rowan-Robinson 1994) and our adopted distance modulus of IC 5152 $(m - M)_0 = 26.6 \pm 0.2$ (Karachentsev et al. 2002), the bright upper limit of supergiant magnitude is set to $m_K = 16.6$ mag. The peak of the M31 globular cluster luminosity function exists near $M_K = -10$ (Barmby et al. 2001), of which the globular cluster system is one of the best studied systems. We have detected 20 star cluster candidates brighter than $K = 16.6$ mag and listed them in Table 2 together with the JHK photometry.

In order to make direct confirmation for these star cluster candidates, we have examined the radial profiles of the candidate clusters with the *HST/WFPC2* F814W image (Karachentsev et al. 2002). Stars on

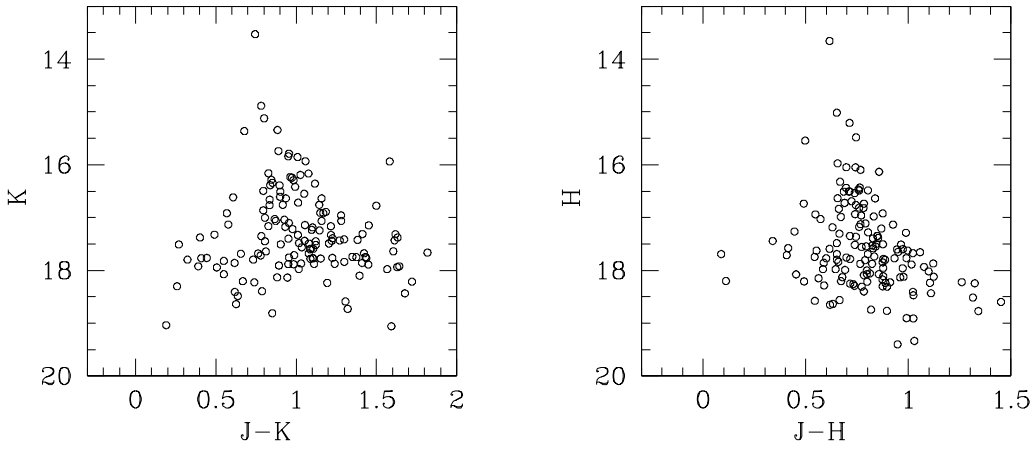

Fig. 2.— The color-magnitude diagrams of all the objects detected in our near-infrared images of IC 5152.

Table 2. The candidated star clusters of IC 5152 ($K \leq$16.6)

ID	X(pixels)	Y(pixels)	K	$J-H$	$H-K$
1	118.19	53.35	16.16	0.67	0.16
2	94.95	62.08	15.84	0.75	0.20
3	142.51	68.44	16.19	0.71	0.31
4	86.76	69.26	16.51	0.69	0.21
5	128.11	77.89	15.79	0.70	0.26
6	62.23	79.72	16.17	0.76	0.32
7	109.94	97.36	16.23	0.76	0.20
8	68.68	103.25	16.42	0.72	0.27
9	152.41	107.21	16.36	0.84	0.28
10	150.45	110.49	16.49	0.66	0.14
11	146.33	116.28	16.34	0.69	0.17
12	150.23	117.03	16.39	0.80	0.09
13	99.46	121.02	16.39	0.76	0.08
14	134.68	113.77	15.12	0.71	0.09
15†	49.62	123.92	15.34	0.75	0.14
16	101.86	149.01	16.29	0.74	0.29
17	171.16	152.84	14.88	0.65	0.13
18	133.78	156.07	15.74	0.66	0.23
19	75.44	159.58	16.55	0.78	0.27
20	30.76	178.70	16.29	0.70	0.15

† : near the H II region #A

Table 3. The young cluster candidates and their reddening values in IC 5152

X(pixels)	Y(pixels)	K	$J-H$	$H-K$	A_V
40.68	29.08	17.86	0.62	0.79	2.5
159.26	105.20	17.92	0.82	0.83	4.5
139.98	115.61	17.19	0.54	0.56	3.0
60.41	119.80	17.43	0.87	0.74	5.6
129.98	192.77	17.42	0.68	0.71	3.7

the *WFPC2* WF3 image (pixel scale of 0.″1) have typically 0.9 pixels of FWHM. On the contrary, our sample of cluster candidates have the FWHM range of 1.5 to 2.6 pixels. Thus, the result suggests that most of the cluster candiates must be genuine star clusters. The young cluster candidates found in the following subsection could not be confirmed due to the heavy reddening in the optical wavelength.

(c) Young Clusters

It is plausible that there are many young star clusters in the star forming galaxy IC 5152. However, it is not easy to identify young clusters only in CMD because of the heavy internal reddenings. Therefore, the $(J-H, H-K)$ two color diagram plotted in Figure 3 is very helpful for this purpose. The suspected young clusters form a sequence in the $(J-H, H-K)$ diagram that parallels the reddening vector while the old clusters are located near the main sequence or giant branch lines given by Bessell & Brett (1988). Five objects with very red colors are detected in Figure 3 and these are identified as compact young clusters forming a sequence that parallels the reddening vector.

The line of sight extinction for each candidate young

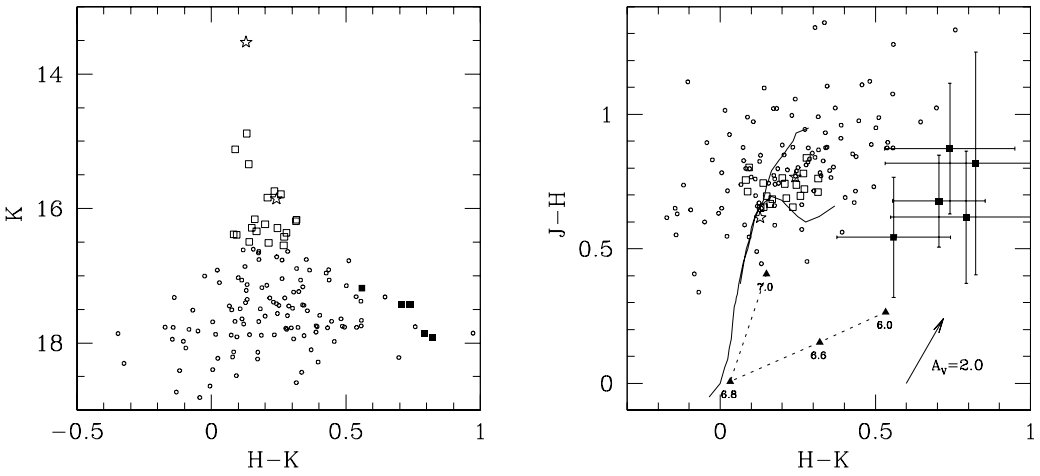

Fig. 3.— $(K, H-K)$ CMD(*left*) and $(J-H, H-K)$ diagram(*right*) of IC 5152. The symbols are "star" : field star, "open squares" : star clusters and "filled squares" : young clusters. The filled triangles mean the theoretical values given by Leitherer et al. (1999) and the labels represent the assumed ages of log t (see text for details). The error bars in the right panel show the estimated uncertainties in the photometric calibration. The solid lines in the right panel show the sequences for solar neighborhood giants (upper line) and dwarfs (lower line) given by Bessell & Brett (1988). The arrow is the reddening vector $E(J-H) = 1.94 \times E(H-K)$ for $A_V = 2$ (Rieke & Lebofsky 1985).

cluster was estimated by extrapolation along the reddening vector to a point midway between the log t(yr)=6.0 and 6.6 models given by Leitherer et al. (1999). The theoretical colors were computed by the $Z = 0.004$ STARBURST99 models with $\alpha = 2.35$, $M_{\rm low} = 1M_{\odot}$, and $M_{\rm up} = 100M_{\odot}$, where Z is the metallicity, α is the exponent of the power law initial mass function, and $M_{\rm low}$ and $M_{\rm up}$ are the low- and high-mass cutoff values, respectively. While the metallicity derived for IC 5152 by Zijlstra & Minniti (1999) is $Z = 0.002$, we have adopted the metallicity of $Z = 0.004$ since the STARBURST99 models calculate only for five fixed values of metallicities.

The photometry result of the candidate young clusters and their reddening values are listed in Table 3. Especially, the young cluster near the H II region #A (X=60.41, Y=119.80) shows heavy reddening ($A_V = 5.6$). Finally the identified objects in the observed field are shown in Figure 4.

IV. SUMMARY

From the analysis of our JHK photometry of IC 5152, we can summarize the followings:

1. We found 20 star cluster candidates based on the distance modulus $(m-M)_0 = 26.6$ and the bright limit of supergiant stars ($M_K = -10.0$) after excluding the foreground stars that are expected from the Galactic star count model of Ratnatunga & Bahcall (1985). And the radial profiles of these candidates on the *HST/WFPC2* image show that the FWHMs of these objects are much larger than those of the typical stars. This confirms that these candidates must be genuine star clusters.

2. The possible young star clusters with heavy internal reddenings are identified in the $(J-H, H-K)$ two color diagram. Total extinction values toward these young clusters are estimated to be $A_V = 2-6$ from the comparison with theoretical values.

We would like to thank the staffs of MSSSO, Australian National University for the use of observing facilities. This research has made use of the NASA/IPAC Extragalactic Database (NED) which is operated by the Jet Propulsion Laboratory, California Institute of Technology, under contract with the National Aeronautics and Space Administration.

REFERENCES

Barmby, P., Huchra, J. P., & Brodie, J. P. 2001, The M31 globular cluster luminosity function, AJ, 121, 1482

Belokurov, V., et al. 2006, A faint new Milky Way satellite in Bootes, ApJ, 647, L111

Bessell, M. S., & Brett, J. M. 1988, *JHKLM* photometry – Standard systems, passbands, and intrinsic colors, PASP, 100, 1134

Burstein, D. A., & Heiles, C. 1984, Reddening estimates for galaxies in the Second Reference Catalog and the Uppsala General Catalog, ApJS, 54, 33

Buyle, P., Michielsen, D., De Rijcke, S., Ott, J. & Dejonghe, H. 2006, The CO content of the Local Group dwarf irregular galaxies IC 5152, UGCA 438, and the Phoenix dwarf, MNRAS, 373, 793

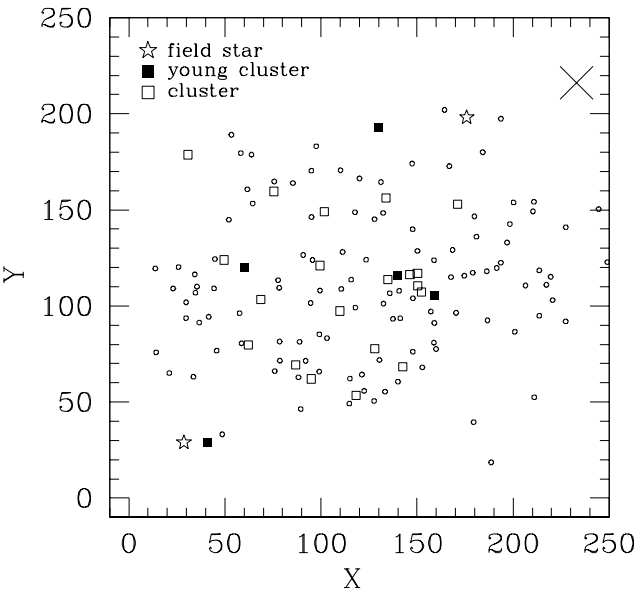

Fig. 4.— The identified objects in the observed field. The symbols are same as in Figure 3, and the X and Y coordinates are in pixel units. The large cross in the upper right part represents the brightest star HD 209142.

Carter, B. S., & Meadows, V. S. 1995, Fainter southern JHK standards suitable for infrared arrays, MNRAS, 276, 734

Cutri, R. M., et al. 2003, The IRSA 2MASS All-Sky Point Source Catalog, http://irsa.ipac.caltech.edu/applications/Gator/

Grebel, E. K. 2000, The star formation history of the Local Group, in Star Formation from the Small to the Large Scale, Proceedings of the 33rd ESLAB symposium, eds. F. Favata, A. Kaas and A. Wilson, (ESA, SP-445:ESA), 87

Hidalgo-Gámez, A. M. & Olofsson, K. 2002, The chemical content of a sample of dwarf irregular galaxies, A&A, 389, 836

Huchtmeier, W., & Richter, O. G. 1986, H I - observations of galaxies in the Kraan-Korteweg – Tammann catalogue of nearby galaxies. I. The data, A&AS, 63, 323

Karachentsev, I. D., Sharina, M. E., Makarov, D. I., Dolphin, A. E., Grebel, E. K., Geisler, D., Guhathakurta, P., Hodge, P. W., Karachentseva, V. E., Sarajedini, A., & Seitzer, P. 2002, The very local Hubble flow, A&A, 389, 812

Leitherer, C., Schaerer, D., Goldader, J. D., Gónzalez Delgado, R. M., Robert, C., Kune, D. F., de Mello, D. F., Devost, D., & Heckman, T. M. 1999, Starburst99: Synthesis Models for Galaxies with Active Star Formation, ApJS, 123, 3

McGregor, P. 1995, Users Manual for the CASPIR on the MSSSO 2.3 m Telescope

Ratnatunga, K. U., & Bahcall, J. N. 1985, Estimated number of field stars toward Galactic globular clusters and Local Group Galaxies, ApJS, 59, 63

Rieke, G. H., & Lebofsky, M. J. 1985, The interstellar extinction law from 1 to 13 microns, ApJ, 288, 618

Rozanski, R., & Rowan-Robinson, M. 1994, The accuracy of the brightest stars in galaxies as distance indicators, MNRAS, 271, 530

Sandage, A. 1986, The redshift-distance relation. IX. Perturbation of the very nearby velocity field by the mass of the Local Group, ApJ, 307, 1

Sandage, A., & Bedke, J. 1985, Candidate galaxies for study of the local velocity field and distance scale using Space Telescope. I. The most easily resolved, AJ, 90, 1992

Skillman, E. D., Kennicutt, R. C., & Hodge, P. W. 1989, Oxygen abundances in nearby dwarf irregular galaxies, ApJ, 347, 875

Stetson, P. B. 1990, On the growth-curve method for calibrating stellar photometry with CCDs, PASP, 102, 932

Stetson, P. B. 1993, Further progress in CCD photometry, in Stellar Photometry, Current Techniques and Future Developments, Proceedings of the IAU Colloquium No. 136, eds. C. J. Butler & I. Elliot(Cambridge University Press: Cambridge), 291

van den Bergh, S. 1994, The outer fringes of the Local Group, AJ, 107, 1328

Willman, B., et al. 2005, ApJ, A new Milky Way dwarf galaxy in Ursa Major, ApJ, 626, L85

Zijlstra, A. A., & Minniti, D. 1999, A dwarf irregular galaxy at the edge of the Local Group: Stellar populations and distance of IC 5152, AJ, 117, 1743

Zucker, D. B., et al. 2004, Andromeda IX: a new dwarf spheroidal satellite of M31, ApJ, 612, L121

Zucker, D. B., et al. 2006a, A new Milky Way dwarf satellite in Canes Venatici, ApJ, 643, L103

Zucker, D. B., et al. 2006b, A curious Milky Way satellite in Ursa Major, ApJ, 650, L41

Zucker, D. B., et al. 2006c, Andromeda X, a new dwarf spheroidal galaxy of M31: Photometry, ApJL, submitted (astro-ph/0601599)